3B2v7.51c GML4.3.1 DSRII : 1338 Prod.Type:COM pp.1–24(col.fig.:4) ED:ShivaKumar PAGN: nmanjunatha SCAN:

ARTICLE IN PRESS

PERGAMON

Deep-Sea Research II ▮ (▮▮▮▮) ▮▮▮–▮▮▮

DEEP-SEA RESEARCH PART II

www.elsevier.com/locate/dsr2

Deep topographic barriers within the Indonesian seas

Arnold L. Gordon[a,*], Claudia F. Giulivi[a], A. Gani Ilahude[b]

[a] *Lamont-Doherty Earth Observatory, Palisades, New York, 10964-8000 USA*

[b] *Pusat Penelitian Oseanografi, LIPI, Jl. Pasir Putih 1, Ancol Timur, Jakarta 14430, Indonesia*

Accepted 10 November 2002

Abstract

Whereas at the surface and at thermocline depth the Indonesian throughflow can weave its way between basins towards the Indian Ocean on a quasi-horizontal plane, at greater depth numerous sills are encountered, resulting in circulation patterns governed by density-driven overflow processes. Pacific water spills over deep topographic barriers into the Sulawesi Sea and into the Seram and Banda seas. The western-most throughflow path flowing through Makassar Strait encounters shallower barriers than does the eastern path. The first barrier encountered by Pacific water directed towards Makassar Strait is the 1350-m deep Sangihe Ridge, providing access to the Sulawesi Sea. The 680-m deep Dewakang Sill separating the southern Makassar Strait from the Flores Sea is a more formidable barrier. Along the eastern path, Pacific water must flow over the 1940 m barrier of the Lifamatola Passage before passing into the deep levels of the Seram and Banda Seas. The deepest barrier encountered by both the western and eastern paths to the Indian Ocean is the 1300–1450 m (perhaps as deep as 1500 m) sill of the Sunda Arc near Timor. The Savu Sea while connected to the Banda Sea down to 2000 m depth, is closed to the Indian Ocean at a depth shallower than the Timor Sill. The density-driven overflows force upwelling of resident waters within the confines of the basins, which is balanced by diapycnal mixing, resulting in an exponential deep-water temperature profile. A scale depth ($Z^* = K_z/w$) of 420–530 m is characteristic of the 300–1500 m depth range, with values closer to 600 m for the deeper water column. The upwelled water within the confines of the Banda Sea, once over the confining sill of the Sunda Arc, may contribute 1.8–2.3 Sv the interocean throughflow.

© 2003 Elsevier Science Ltd. All rights reserved.

1. Introduction

As part of the Arlindo Project, a joint oceanographic research endeavor of Indonesia and the United States, profiles of temperature, salinity and oxygen were obtained within the Indonesia seas with CTD equipment and water samples for salinity and oxygen standardization (Fig. 1). The Arlindo CTD stations extend to the sea floor or to 3000 decibars (dbar; the shallower of the two), were obtained during four periods: using the Indonesian research vessel Baruna Jaya I, during the South East Monsoon of 1993 (August and September) and reoccupied during the North West Monsoon of 1994 (January and March); additional CTD stations were obtained from Baruna Jaya IV in November–December 1996 and February 1998. The Arlindo data were used to investigate the water mass composition and mixing

*Corresponding author. Tel.: +1-845-365-8325; fax: +1-845-365-8157.

E-mail address: claudiag@ldeo.columbia.edu (A.L. Gordon).

0967-0645/03/$ - see front matter © 2003 Elsevier Science Ltd. All rights reserved.
doi:10.1016/S0967-0645(03)00053-5

UNCORRECTED PROOF

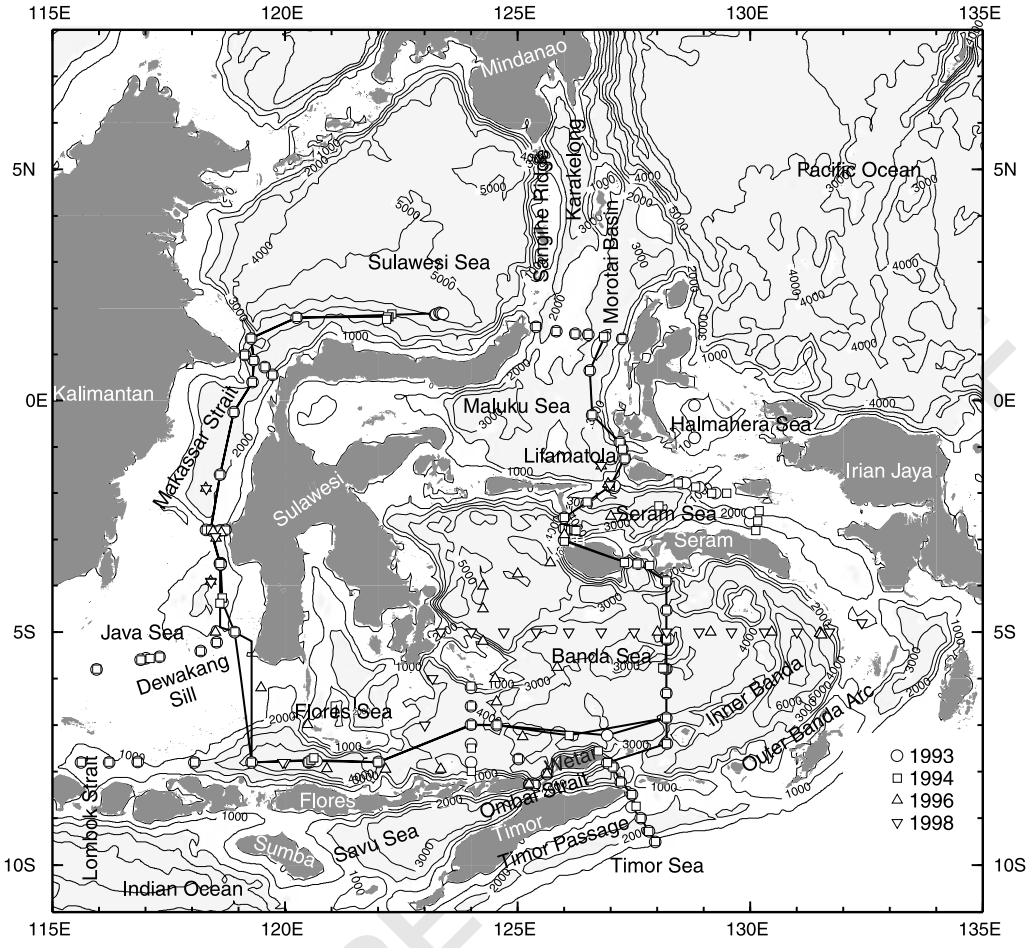

Fig. 1. Map showing the major bathymetric features of the Indonesian Seas and the position of CTD stations taken during the Arlindo cruises. Connected symbols by a solid black line represent the western and eastern sections shown in Figs. 5 and 6. Sea floor bathymetry (contours every 1000 m, gray shading for depths deeper than 2000 m) has been extracted from Smith and Sandwell (1997).

within the thermocline of the Indonesian Seas (Gordon, 1995; Gordon and Fine, 1996; Ilahude and Gordon, 1996a, b; Ffield and Gordon, 1996). The objectives of this paper are to combine the Arlindo data with archived data (Conkright et al., 1998) to: (1) determine the effective sill depths of the ridges segmenting the primary Indonesian basins, and (2) investigate the stratification within the intermediate and deep-water layers of the Indonesian Seas. Correct sill depths are essential for proper model simulation of stratification and interocean transport characteristic of the Indonesian Seas (Gordon and McClean, 1999).

Whereas the surface and thermocline water component of the Indonesian throughflow can weave its way between the multitude of Indonesian Islands towards the Indian Ocean on an approximate horizontal plane, without significant impedance by topography, below thermocline depths numerous sills are encountered. This induces deep circulation patterns governed by density-driven overflow processes, in which resident deep water, continuously made less dense by downward eddy diffusion of buoyancy, is displaced upward. Overflow of Pacific water into the northern Banda Sea through the Lifamatola Passage with a sill depth

near 1940 m is a well-known example of such a process within the Indonesian seas (Wyrtki, 1961; Broecker et al., 1986; Van Aken et al., 1988). Based on a 3-month current meter record, from January to March 1985, in the deep axis of Lifamatola Passage the estimated overflow transport through the Lifamatola Passage deeper than 1500 m is 1.5 Sv ($1\,Sv = 10^6\,m^3/s$), which is sufficient to force a 29-year residence time for the Banda Sea below 1500 m, corresponding to an upwelling across a 1500 m horizon of 75 m/year or 2.38×10^{-6} m/s (Van Aken et al., 1988, 1991). This overflow speed of Van Aken et al. (1988) is about 3 times (residence time 1/3) that found by Broecker et al. (1986) based on a 1-month current meter record obtained in Lifamatola Passage in January/February 1976. Postma and Mook (1988) using Carbon-14 (^{14}C) find a flushing rate in the eastern Indonesian seas of 10–140 years, with values closer to 10 years in the western and northern Banda Sea and Seram Sea, and a basin-wide average of 25 years. Wyrtki (1961) noted that the relatively high oxygen within the deep waters suggests good ventilation of these waters, but cautioned that it may also be the result of very low rates of oxygen consumption.

Makassar contribution to the throughflow is blocked by the Dewakang Sill, named after the local Island group, with a 680-m sill depth, as determined from depths shown on Indonesian navigation charts (Ilahude and Gordon, 1996a). Throughflow contribution below 680 m must be derived solely from the eastern throughflow channels including the Lifamatola Passage overflow to the deep Banda Sea. From March 1992 to April 1993 the average transport within the Timor Passage (south of Timor) measured during the JADE French–Indonesian program, from the surface to 1250 m is 3.4–5.3 Sv (Molcard et al., 1996). Of this amount, 1.2–1.5 Sv occurs between 680 and 1250 m. An additional transport of 0.5 Sv is estimated between 1250 and 1550 m, but this is believed to be a return of Indian Ocean deep water that passed to the east within the deep channel axis (about 1800 m), inhibited from entering the Banda Sea which has a approximate sill depth of 1450 m (Van Aken et al., 1988). Molcard et al. (2001) report on the results of a JADE 1-year mooring beginning in late November 1995 in Ombai Strait, a 30-km wide and 3250 m deep passage separating Timor from Islands to its immediate north. The estimated transport is 4–6 Sv. Between 680 and 1200 m the transport is estimated as 0.6 and 0.8 Sv. From the JADE data we may expect that the total throughflow below the Makassar sill depth into the Indian Ocean is 1.8–2.3 Sv. All the connections between the interior Indonesian Seas and the Indian Ocean to the west of Timor are shallower than 680 m. The Van Aken et al. (1988) transport of 1.5 Sv deeper than 1500 m can explain roughly all but 0.5 Sv of the >680 m export to the Indian Ocean. Noting the short time span of the Lifamatola moorings, an additional 0.5 Sv of Lifamatola Passage overflow required to close the deep throughflow budget, is reasonable. Of course the Timor Passage, Ombai Strait and Lifamatola Passage measurements were made at different times, and the assumptions of a steady-state system does not necessarily apply in this case, but the near balance is instructive. Van Bennekom (1988) using silicate distribution surmise that some of the water leaving the Banda Sea near 1000 m depth just to the east of Sunda chain Island of Wetar then turn eastward (therefore do not pass across the JADE moorings) to flow along the Outer Banda Arc (Fig. 1), thus forming a large re-circulating loop.

The Timor Passage and Ombai Strait total transport between the sea surface and 680 m from the Molcard et al. (1996; 2001) JADE results is between 5.6 and 9.0 Sv. Adding the estimated Lombok Strait transport of 1.7 Sv (Murray and Arief, 1988, measured in 1985) we arrive at 7.3–10.7 Sv, which is not significantly different than the Makassar Strait transport of 9.3 ± 2.5 Sv (Gordon et al., 1999). This suggests that the Makassar throughflow may provide all of the export to the Indian Ocean for the water column from the sea surface to 680 m, with the Lifamatola Passage overflow providing the deeper throughflow.

The Arlindo and JADE Helium-3 (^3He) data are used to trace deep-water movements within the Indonesian seas (Top et al., 1997). ^3He sources in the Sulawesi Sea and in Makassar Strait are found, but these are prevented from spreading into the

UNCORRECTED PROOF

Banda Sea and Indian Ocean by blocking sills. A major mantle source is identified below 2000 m in the Banda and Flores Seas. Higher-than-ambient ^{3}He on the Indian Ocean side of the Lesser Sunda Island chain indicates a deep outflow of Flores and Banda Sea water into the Indian Ocean near 1300 m.

2. The topographic divides

The depths of the critical sills that govern deep inter-basin exchange of water masses within the Indonesian seas can be estimated by comparing the profiles of temperature on either side of the topographic barrier. This classic oceanographic method provides what is called the thermometric sill depth. It is determined by comparing the bottom temperature on the overflow side of a sill with the temperature profile on the upstream side of the sill. Effective sill depths also can be estimated from other parameters, such as salinity or oxygen, but generally the temperature profile has the best dynamic range and affords the best estimate of sill depths. However, there are measurement errors and real temporal variability of the temperature (and other parameter) profiles. The accuracy of a thermometric or effective sill depth depends on the scatter of points defining the mean profile, which generally is larger for the shallower levels. In the discussion to follow the scatter shown in Figs. 2 and 3 allows an estimate of sill depth to roughly 5–10% of the sill depth for sills deeper than 1000 m, 10–20% for sills shallower than 1000 m. The thermometric or effective depth does not need to be equal to the depth of the deepest saddle of a ridge. The overflow water is expected to be a blend of characteristics over a layer of the inflowing water column from the deepest sill up to some shallower depth. The thickness of the overflow layer is determined by the sill topography (for example, a broad u-shaped gap versus a more restrictive v-shaped gap) and mixing, such as entrainment and shear induced turbulence, including the effects of internal wave at the sill. The effective sill depth is expected to be somewhat shallower than the actual deepest path between basins as might be determined by a bathymetric survey.

The primary deep sills between the Pacific and Indonesian seas within the northern Indonesian seas are:

1. Sangihe Ridge stretching from Sulawesi to Mindanao, which limits deep water access to the Sulawesi Sea and Makassar Strait;
2. Halmahera Sea sill depth controlling direct access of South Pacific water to the Indonesian Seas; and
3. Lifamatola Passage, which links the Maluku Sea to the Banda Sea.

The Inner and the Outer Banda Arcs cut by numerous deep channels leading to passages both north (Ombai Passage) and south (Timor Passage) of Timor separate the Indian Ocean from the southern Indonesian Seas. The Torres Strait is the shallow connection of the South Pacific to the Indonesian Seas between Australia and New Guinea. It is less than 10 m deep with the presence of numerous Islands and reefs. From 5 months of current observations, Wolanski et al. (1988) found a strong tidal flow, but no evidence of a mean flow through Torres Strait.

The Arlindo data is limited to the upper 3000 m, deep enough to reach the sill depths, but not deep enough to resolve the deep-water properties on the overflow side of the sill, as required to estimate effective sill depths. Therefore, archived regional data (Conkright et al., 1998) are added to the Arlindo stations to determine the controlling sill depths. Effective sill depths are determined by matching the bottom potential temperature and salinity point within the enclosed basin with the stratification on the open ocean side of the sill. The water within the enclosed basins, but below sill depth is made more buoyant than the overflow water by vertical mixing; this process allows open-ocean water at the sill depth to continually renew the bottom water of the enclosed basin. In the mean, diapycnal mixing rate within the isolated basin essentially determines the rate of renewal of deep basin water. Transient effects at the sill may lead to sporadic overflow.

UNCORRECTED PROOF

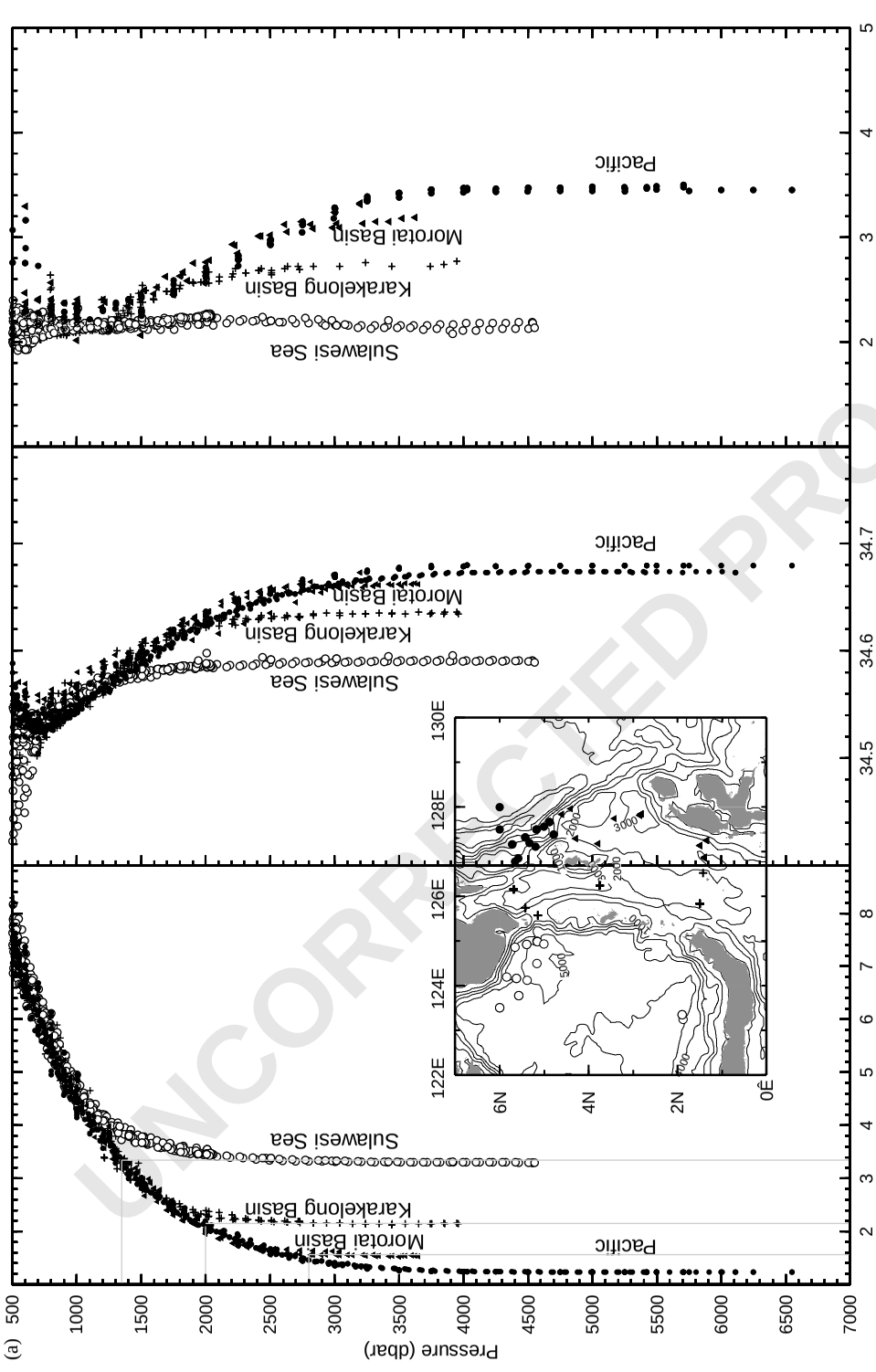

Fig. 2. Temperature, salinity and oxygen profiles defining the controlling sill depths between the northern Indonesian Seas (open symbols) and Pacific Ocean (solid symbols) based on Arlindo data and archived regional data (Conkright et al., 1998): (a) Sangihe Ridge, sill depth of 1350 m; (b) Halmahera Sea, sill depth of 580 m and (c) Lifamatola Passage, sill depth of 1650 m. The inset maps show the location of the data and sea floor bathymetry (contours every 1000 m, gray shading for depths deeper than 2000 m). Besides Arlindo data the following data were used (ship names are in italics; expedition names are in capital letters; in parenthesis is the number of stations): INDLEG 7 (6); SNELLIUS 2 (20); WEPOCS (13); *Hakuho Maru* (1); *Kaiyo* (13); *Prilir* (3); *Ryofu Maru* (20); *Samudera* (23); *Xiang Yan Hong* (4).

UNCORRECTED PROOF

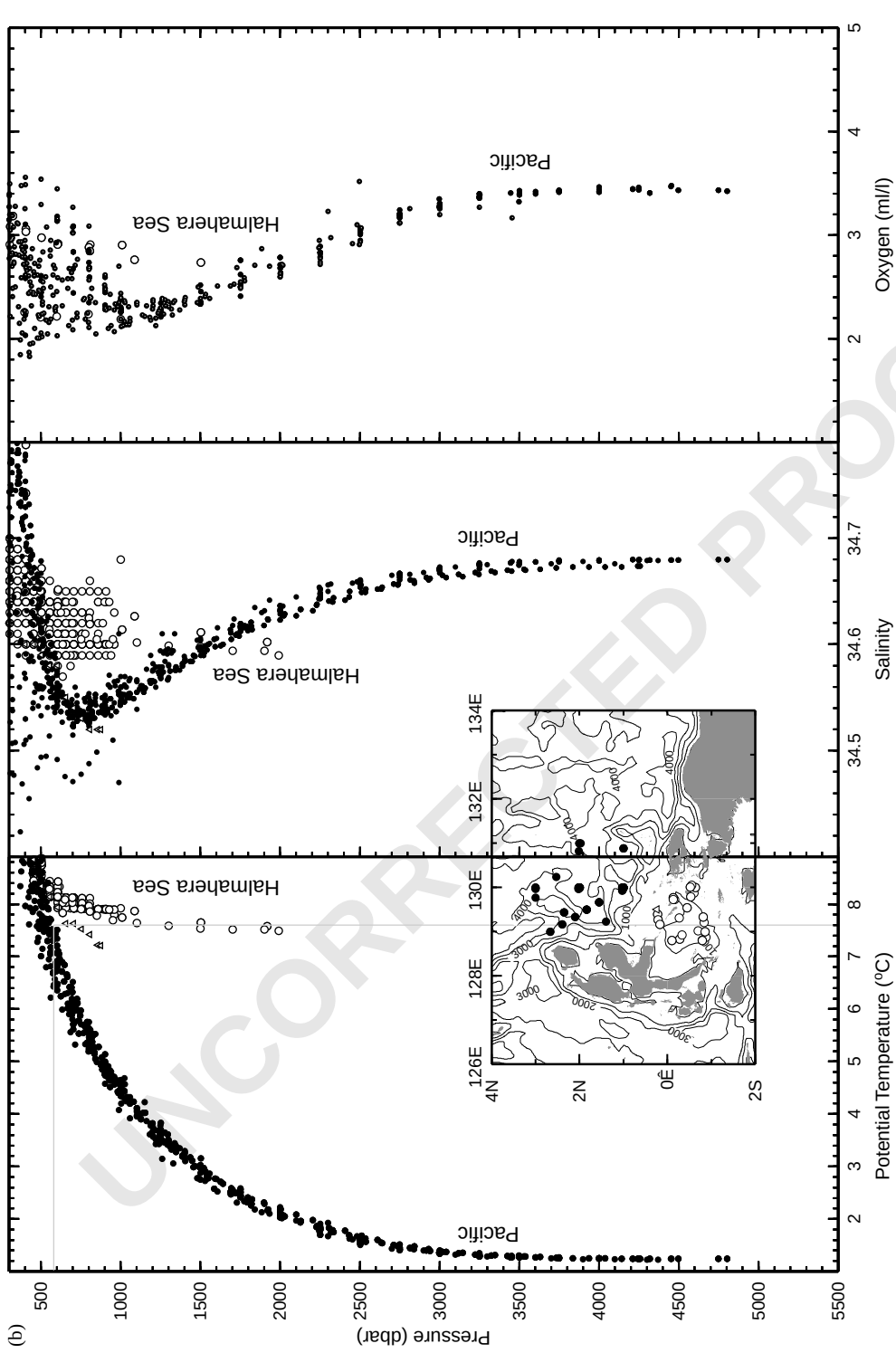

Fig. 2 (*continued*).

UNCORRECTED PROOF

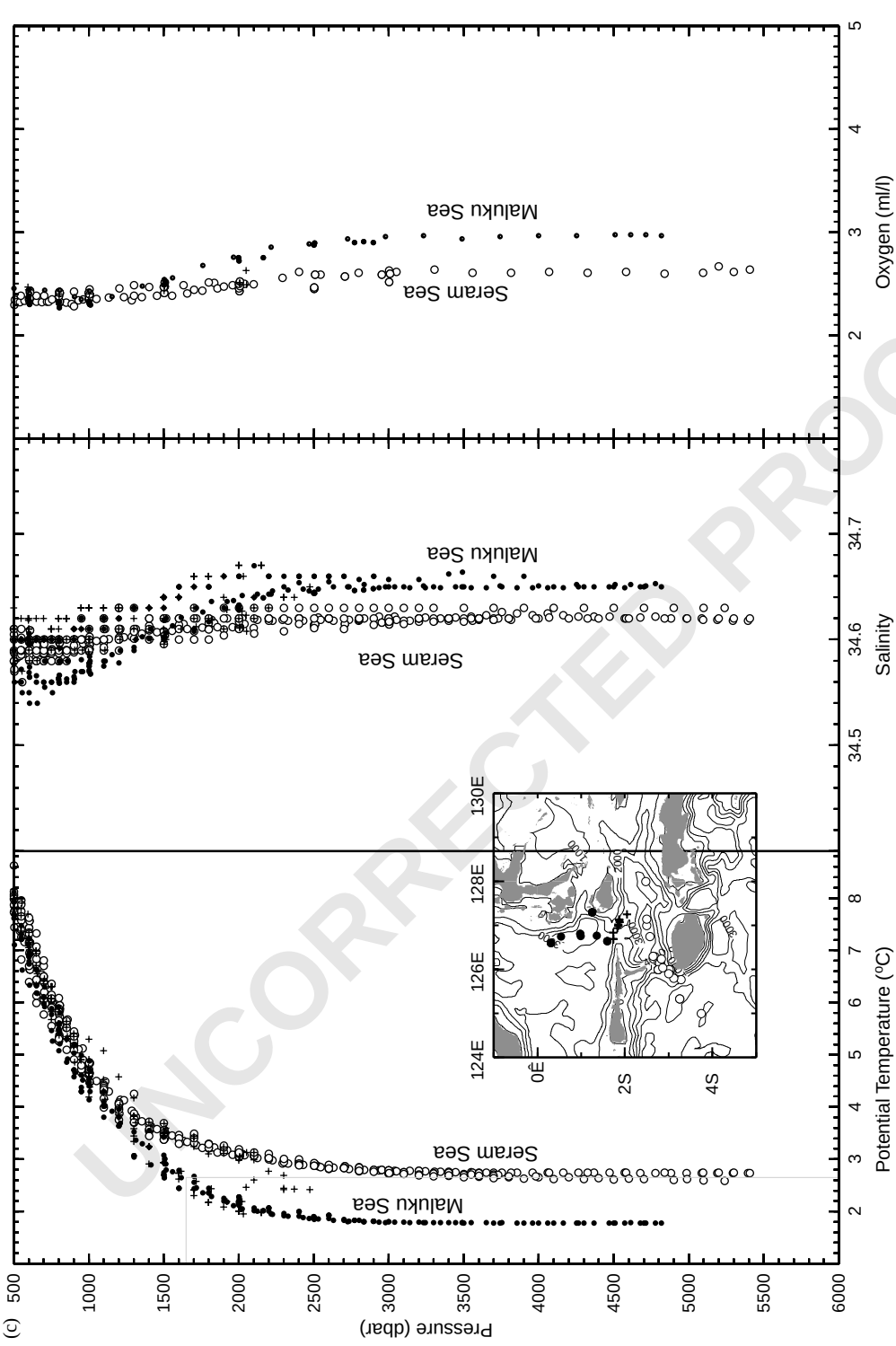

UNCORRECTED PROOF

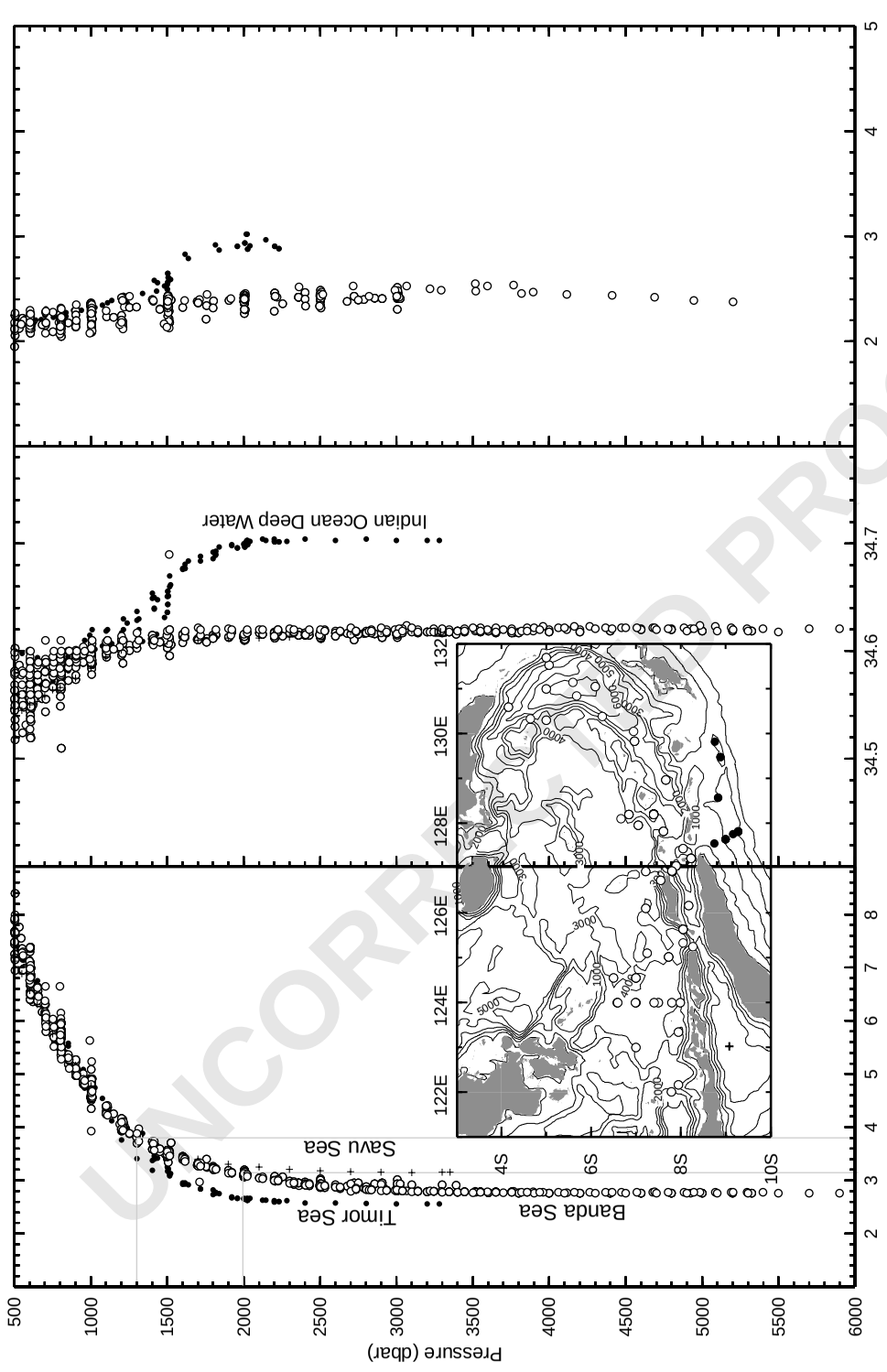

Fig. 3. Temperature, salinity and oxygen profiles across the inner and outer Sunda Arcs between the Banda Sea (open symbols) and Indian Ocean (Timor Sea) (solid symbols) based on Arlindo data and archived regional data (Conkright et al., 1998). Besides Arlindo data the following data were used (ship names are in italics; expedition names are in capital letters; in parenthesis is the number of stations): INDLEG 7 (5); SNELLIUS 2 (8); *Jalanidhi* (6); *Samudera* (1).

UNCORRECTED PROOF

2.1. Northern access

Sangihe Ridge: The Sangihe Ridge spans the distance between the northeastern tip of Sulawesi to the southern end of Mindanao (Fig. 2a). It is broken by three channels, which Mammericks et al. (1976) show to lie each between 1000 and 1500 m. We name each after the adjacent island: the Kawio sill in the north at 5°10′N and two sills in the southern end of the ridge: Biaro sill at 2°00′N and the Ulu Siau sill at 2°30′N. The comparison of the stratification in the Sulawesi Sea with that to the Pacific Ocean side of the ridge (Fig. 2) indicates that at depths deeper than roughly 1000 profiles of potential temperature, salinity and oxygen from opposites sides of the ridge diverge from each other with increasing depth. This indicates restricted communication between the water bodies on either side of the ridge below 1000 m. The bottom water (potential temperature of 3.34°C and salinity of 34.59) in the Sulawesi Sea near 4500 m matches the Pacific values east of the Sangihe Ridge at a depth of 1350 m. Therefore, 1350 m is assigned as the depth of the effective sill depth across the Sangihe Ridge. The Sulawesi bottom water oxygen is slightly lower, 0.15 ml/l, than the oxygen concentrations on the Pacific side of the effective sill. This oxygen decrease is governed by the residence time of Sulawesi bottom water. The data are not sufficient to determine which sill is the primary pathway. Entry into the Sulawesi Sea does not insure spreading at depth into the Flores and Banda Seas, because in the southern Makassar Strait the Dewakang Sill near 680 m (and Ilahude and Gordon, 1996a; Waworuntu et al., 2000) blocks all but the upper layers to free communication with the Flores Sea.

Differences in the profiles that are situated in the Karakelong Basin between the Sangihe Ridge and Karakelong Ridge (see Fig. 1; named for the Island near 4°N, 126.6°E; +symbol on Fig. 2a) are observed below a depth of 1700 m (Fig. 2a). The stations in that basin indicate isolation from the open Pacific Ocean below the effective sill depth of 2000 m. East of Karakelong Ridge is the Morotai Basin that leads into the Maluku Sea (see Fig. 1; stations denoted by a solid in Fig. 2a) with an effective sill depth of 2800 m separating it from the open Pacific Ocean.

Halmahera Sea: The Halmahera Sea is exposed at its northern end to the South Pacific water advected into the region by the New Guinea Coastal Current (Gordon, 1995; Ilahude and Gordon, 1996a, b). The South Pacific water column may spread into the southern Halmahera Sea across a sill near 0.5°N. The salinity and oxygen stratification do not display enough range amid the scatter to help define a sill depth, but the temperature field does a bit better (Fig. 2b). The Halmahera thermal stratification deviates from the Pacific Ocean with increasing depth below 490 m. Bottom-water potential temperature of 7.6°C and salinity of 34.6 in the Halmahera Sea suggest complete blockage near 580 m. Bottom water at near 2000 m is matched by bottom water near 800 m (Fig. 2b), probably just to the overflow side of the effective sill. The shallow Halmahera Sea sill allows saline South Pacific lower thermocline water to enter the Seram Sea (Ilahude and Gordon, 1996a, b), but prohibits deeper water from entering the Indonesian seas, which have access to the interior seas only through the Sulawesi and Maluku Seas, with the Sulawesi pathway blocked near 680 m by the sill in the southern Makassar Strait.

Lifamatola Passage: The Lifamatola Passage is the deepest entry passage for Pacific water into the interior Indonesian seas. A sill depth of 1940 m at 1.81°S, 126.95°E has been determined by careful bathymetric survey (Van Aken et al., 1988). Water profiles (Fig. 2c) reveal that deviation occurs at depths greater than approximately 1400 m, which may be taken as the depth at which restriction of free access begins. Comparison of bottom water in the Seram Sea (2.65°C and 34.62°C) with the Maluku Sea water column suggests an effective sill depth at 1650 m, about 300 m shallower than the surveyed sill depth. The shallow sill relative to the bathymetric survey is likely a consequence of strong mixing due to internal wave energy at the sill (Van Aken et al., 1988; Ffield and Gordon, 1996), which act to dilute the sill depth water with overlying warmer water before descending to the floor of the Seram Sea. A sill depth of 1940 m would produce Seram Sea bottom water potential

UNCORRECTED PROOF

temperature of 2.20°C, 0.45°C colder than observed, if the Lifamatola Passage overflow were laminar. The Seram Sea bottom oxygen is only 0.10 ml/l, slightly lower than the Maluku Sea oxygen at the water property determined sill depth. As the Lifamatola Passage is the deepest passage connecting the Pacific Ocean to the Indonesian Sea, it provides all of the bottom water of the expansive Seram, Banda and Flores seas. The Seram Sea is a relatively small basin (a vestibule to the Banda Sea), with an expected short deep residence time. Postma and Mook (1988), using ^{14}C, estimated the residence time of deep water in the Seram Sea and northern Banda Sea as less than 10 years.

2.2. Southern access

Timor Sea Sill: The deepest link between the Indian Ocean and Indonesian Seas and the majority of export of Indonesia Sea water occurs in the vicinity of Timor involving an array of passages along the Timor Passage and across the Outer Banda Arc (see Mammericks et al., 1976). Secondary export of water to the Indian Ocean also occurs in Lombok Strait, which has a sill depth of about 300 m (Murray and Arief, 1988; Murray et al., 1990). Fieux et al (1996) state that the sill depth near Timor is between 1200 and 1300 m. Van Aken et al. (1988) found a sill near 7.5°S and 132.3°E of 1450 m. As these are both shallower than the Lifamatola Passage, the southern access passages are not the controlling sill for renewal of deep water in the Banda Sea. Therefore, comparison of bottom water on the overflow side to the upstream profiles does not define an effective sill depth; however, they do fix the limits of the sill depth limiting exchange of waters between the Banda Sea and the Indian Ocean. Within the Timor Sea (solid symbols in Fig. 3) divergence of the temperature, salinity and oxygen profiles relative to the Banda Sea stratification is first noticed at 1300 m (near 3.8°C, 34.62, 2.4 ml/l), though more striking below 1500 m. This indicates that below 1300 m, communication between the Banda Sea and Timor Sea is restricted. The cooler, more saline and better oxygenated deep water in Timor Passage below 1500 m is derived from the Indian Ocean (Fieux et al., 1996). Available data suggest that exchange between the Banda and Timor Seas becomes increasingly restricted below 1300 m. Exchange is blocked below 1450 m or perhaps as deep as 1500 m.

Table 1
Sill depths (see Fig. 1 for locations)[a]

Sill	Separating	Sill depth (m)
Sangihe Ridge	Sulawesi—Pacific	1350
Karakelong Ridge	Karakelong—Pacific	2000
Morotai Basin	Maluku—Pacific	2800
Halmahera Sea	Seram—Pacific	580
Lifamatola Passage	Maluku—Banda	1940
Lombok Strait	Flores—Indian	300
Timor Sea	Banda—Indian	1300–1500

[a] Accuracy of the sill depth determinations is estimated to be 5–10% of the sill depth for sills deeper than 1000 m, 10–20% for sills shallower than 1000 m.

The Savu Sea profile (the + symbol on Fig. 3) is warmer than the Banda Sea profile below 1900–2000 m, this is indicative of a sill of approximately that depth between these two seas. However, the lack of the cooler deep Indian Ocean water in the Savu Sea indicates that the connection of the Savu Sea to the open Indian Ocean is shallower than the 1300 m sill depth of the Timor Sea (Table 1).

3. Deep-water upwelling

Van Aken et al. (1988, 1991) investigated the exponential form of the temperature, oxygen, phosphate, silica and ^{14}C profiles in the deep Banda Sea. They noted that the overflow from the Lifamatola Passage has no other escape route than upwelling to the depth of the outflow sill (1300–1500 m, see above) into the Indian Ocean. They explored the Munk abyssal recipe (Munk, 1966) of vertical balance of upwelling, w, to the kinematic vertical mixing coefficient, K_z (the diffusivity divided by the water density) for the Banda Sea. They found a relatively large K_z of $13.0 \times 10^{-4}\,m^2/s$, which they attributed to tidally driven boundary-layer mixing. For comparison we now determine the Z^* (scale height) for the Arlindo CTD data in the deep Banda and Seram Seas for the

UNCORRECTED PROOF

Table 2
Scale height of deep water in the Banda and Seram seas below 1300 m

Parameter	Western Banda	Central Banda	Eastern Banda	Seram
Number of profiles	7	11	5	9
Z^* (m)[a]	582	542	526	608
Std (m)[b]	72	92	57	160
w (m/s)[c]	$2.38 \times 10-6$	$2.38 \times 10-6$	$2.38 \times 10-6$	$2.38 \times 10-6$
K_z (m^2/s)[d]	13.9×10^{-4}	12.9×10^{-4}	12.5×10^{-4}	14.5×10^{-4}

[a] Scale height in meters.
[b] Standard deviation in meters.
[c] w = vertical velocity, m/s. The value is taken from Van Aken et al. (1991) for the upwelling velocity across the top of the confined Banda Sea
[d] K_z = vertical eddy mixing coefficient.

UNCORRECTED PROOF

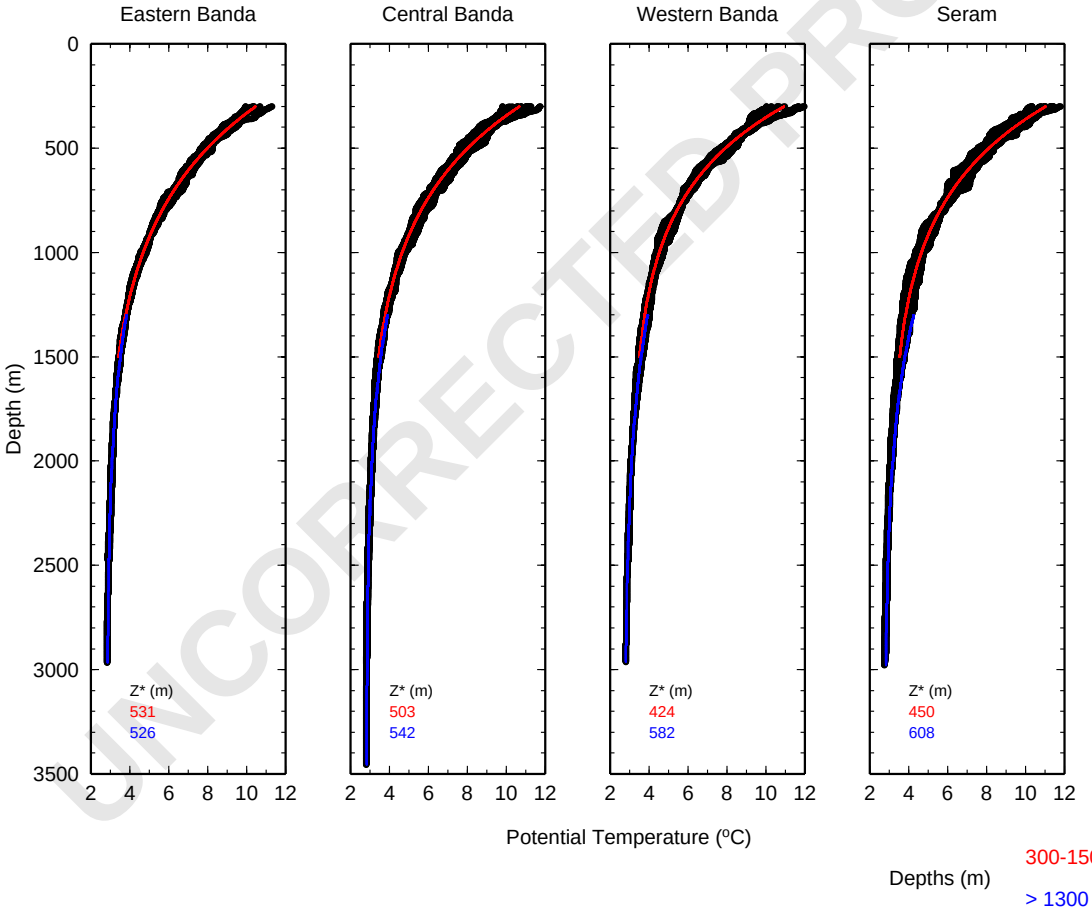

Fig. 4. Temperature profiles for the Banda and Seram Seas based on Arlindo 1993, 1996 and 1998 data. Solid black dots for the observations, the red line indicates the exponential fit according to Eq. (1) (see text) for data between 300 and 1500 m depths (red) and for depths deeper than 1300 m (blue), also shown respectively in red or blue, $Z^*(K_z/w)$ values.

Table 3
Scale height of deep water in the Banda and Seram seas between 300 and 1500 m

Parameter	Western Banda	Central Banda	Eastern Banda	Seram
Number of profiles	7	11	5	9
Z^*[a]	424	503	531	450
Std[b]	77	88	54	59
w (m/s)[c]	2.38×10^{-6}	2.38×10^{-6}	2.38×10^{-6}	2.38×10^{-6}
K_z (m^2/s)	9.8×10^{-4}	11.6×10^{-4}	13.0×10^{-4}	10.1×10^{-4}
w (m/s)[d]	$1.39 \times 10_{-6}$	1.39×10^{-6}	1.39×10^{-6}	1.39×10^{-6}
K_z (m^2/s)	5.7×10^{-4}	6.8×10^{-4}	7.3×10^{-4}	6.2×10^{-4}
w (m/s)[e]	0.24×10^{-6}	0.21×10^{-6}	0.19×10^{-6}	0.23×10^{-6}
K_z(m^2/s)	1×10^{-4}	1×10^{-4}	1×10^{-4}	1×10^{-4}

[a] Scale height in meters.
[b] Standard deviation in meters.
[c] Determination of K_z from the Z^* value using the deep upwelling velocity required to compensating the Lifamatola overflow (Van Aken et al., 1991).
[d] Determination of K_z from the Z^* value using the Ekman-induced upwelling in Banda Sea (Gordon and Susanto, 2001).
[e] Determination of vertical velocity using the canonical vertical mixing coefficient of 10^{-4} m^2/s.

simple one-dimensional vertical balance

$$\theta = \theta_0 \exp^{-Z/Z^*}, \quad (1)$$

$$Z^* = K_z/w. \quad (2)$$

For the Arlindo temperature data deeper than 1300 m for those stations that reach to at least 2000 m, the Z^* was determined for the western, central, eastern Banda Sea and for the Seram Sea (Table 2; Fig. 4). The regional average Z^* is 565 m. Van Aken et al. (1991) calculated Z^* of 560 m. Wyrtki (1961) also noted the exponential nature of the temperature profile below 1500 m within the Banda Sea, but arrived at a larger value of Z^* (714 m; converted from the value in Table 8 of Wyrtki, 1961). Using the upwelling rate of 2.38×10^{-6} m/s across 1500 m that Van Aken et al. (1991) determined from the Lifamatola overflow rate, the K_z value derived from the Arlindo data in the Banda and Seram Seas is 13.3×10^{-4} m^2/s, essentially the same as the value determined by Van Aken et al. (1991). This value represents a regional average. Most of the mixing is expected to be accomplished along the sidewalls. Based on near bottom Radon profiles in the Banda Sea the K_z is found to vary from 46 to 64×10^{-4} m^2/s, reaching 83–2000×10^{-4} m^2/s over rough topography and sills (Berger et al., 1988), with similar values found from the deep silicate distribution (Van Bennekom, 1988).

The regional variability of K_z, highest in the Seram Sea and in the western Banda Sea agree with the spatial variability of the ^{14}C derived deep-water residence time of Postma and Mook (1988), lower residence time for areas of greater vertical mixing. However, in view of the relatively large standard deviations of the Z^* determinations between the profiles used in the calculations, these spatial variations are not significant.

Fig. 5. Western throughflow pathway. Vertical sections: (a) contours of potential temperature combining 1993 and 1994 Arlindo data; the inset map show the location of the section based on the Arlindo data and in small solid circles the location of the archived data; (b) upper panel: contours of salinity only for 1993 Arlindo data; the inset potential temperature versus salinity for both 1993 and 1994 Arlindo data; (c) contours of salinity for the upper 2500 m of 1994 Arlindo data; (d) contours of oxygen (ml/l) combining 1993 and 1994 Arlindo data, the inset, potential temperature versus oxygen for both 1993 and 1994 Arlindo data. The bottom topography along the section is generalized to show only the major basins and topographic barriers. The values shown in most of deep basins represent a spatial/temporal average of archived data (Conkright et al., 1998) found within 50 km from the cruise track. For all sections solid symbols represent Arlindo 1993 data and open symbols, Arlindo 1994 data.

UNCORRECTED PROOF

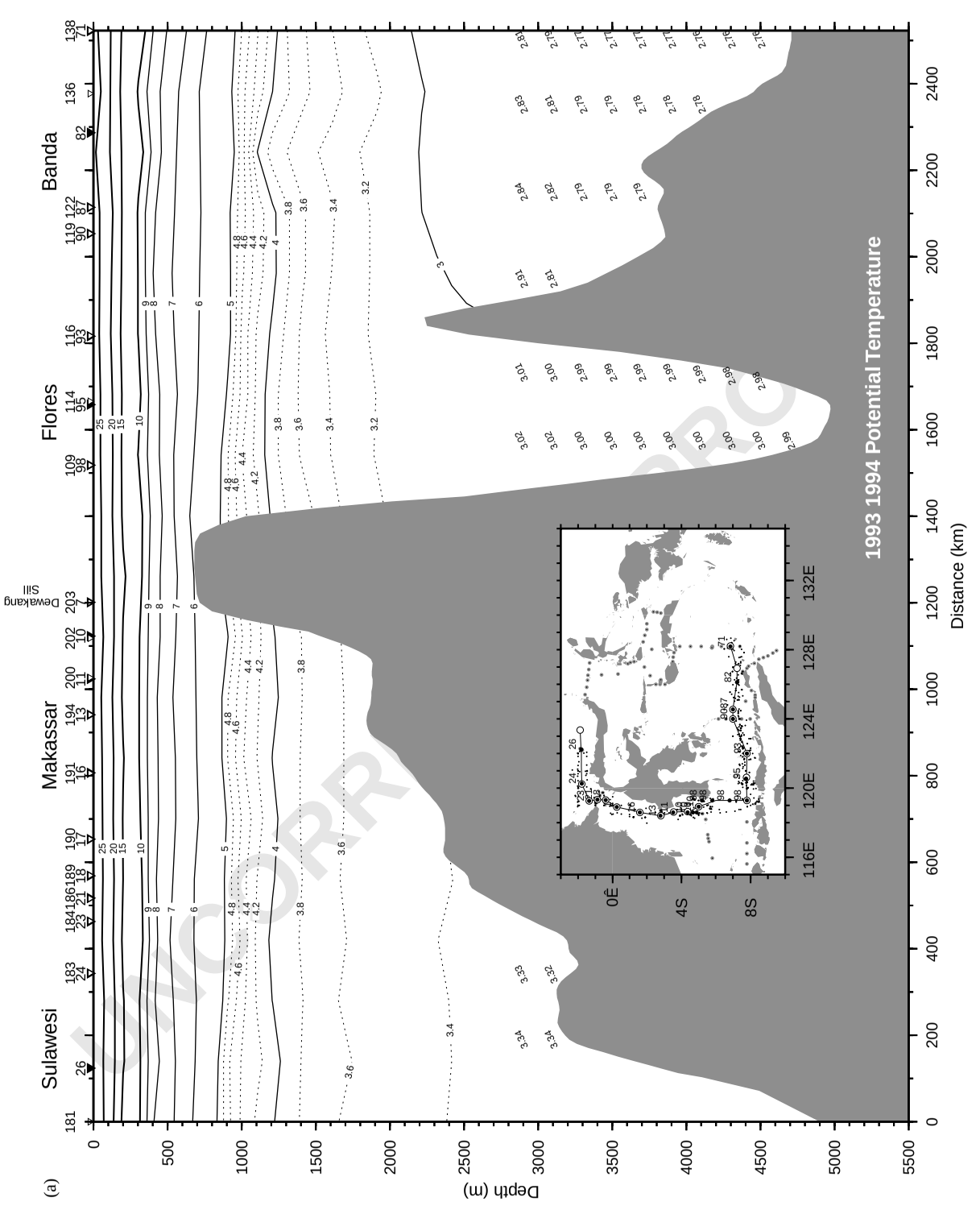
1993 1994 Potential Temperature
Distance (km)
Depth (m)
(a)
Sulawesi
Makassar
Flores
Banda
Dewakang Sill
116E
120E
124E
128E
132E
0Ê
4S
8S

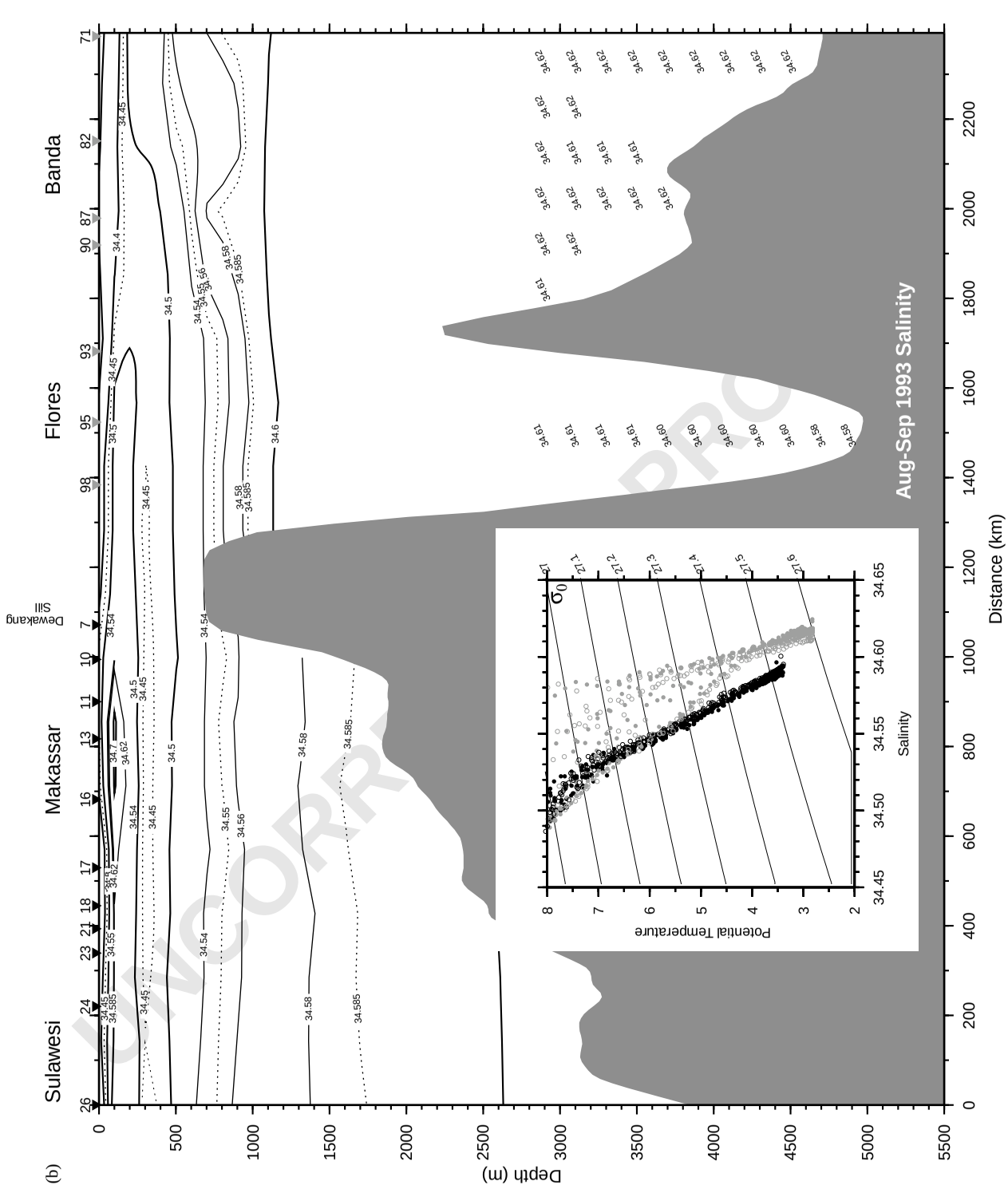

Fig. 5 (*continued*).

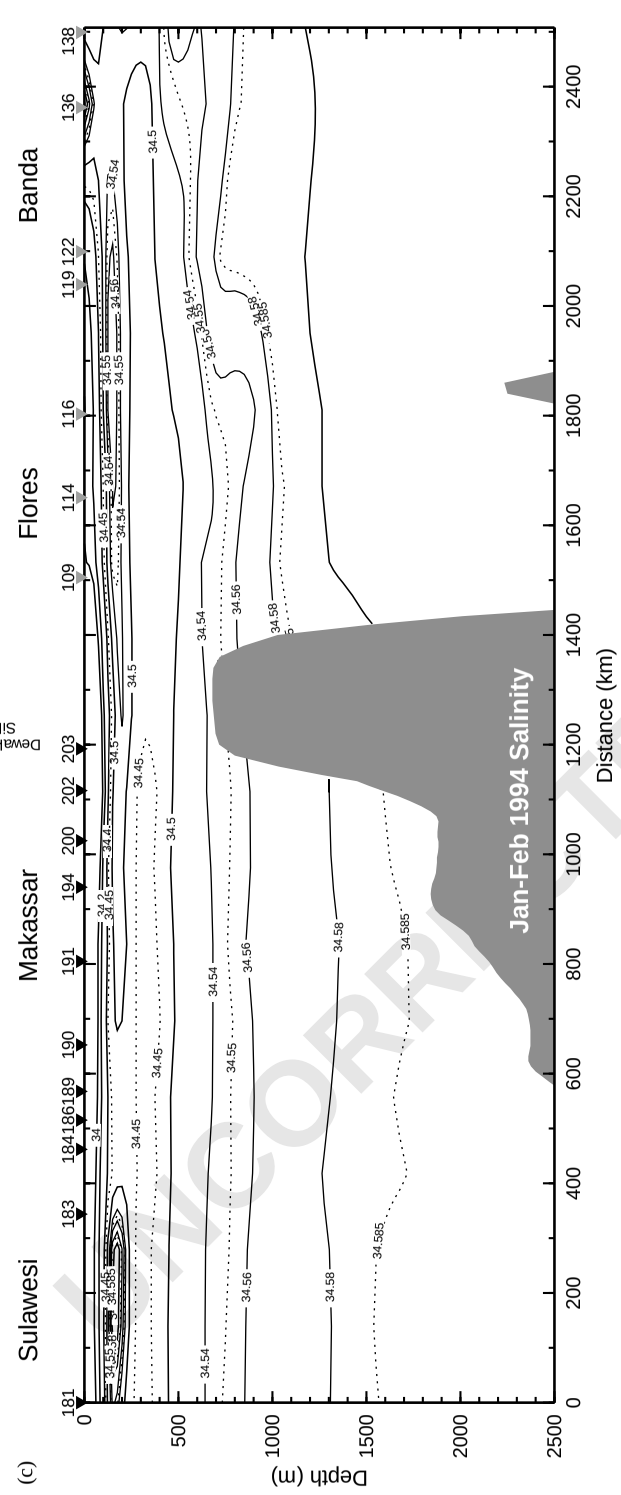

Fig. 5 (*continued*).

UNCORRECTED PROOF

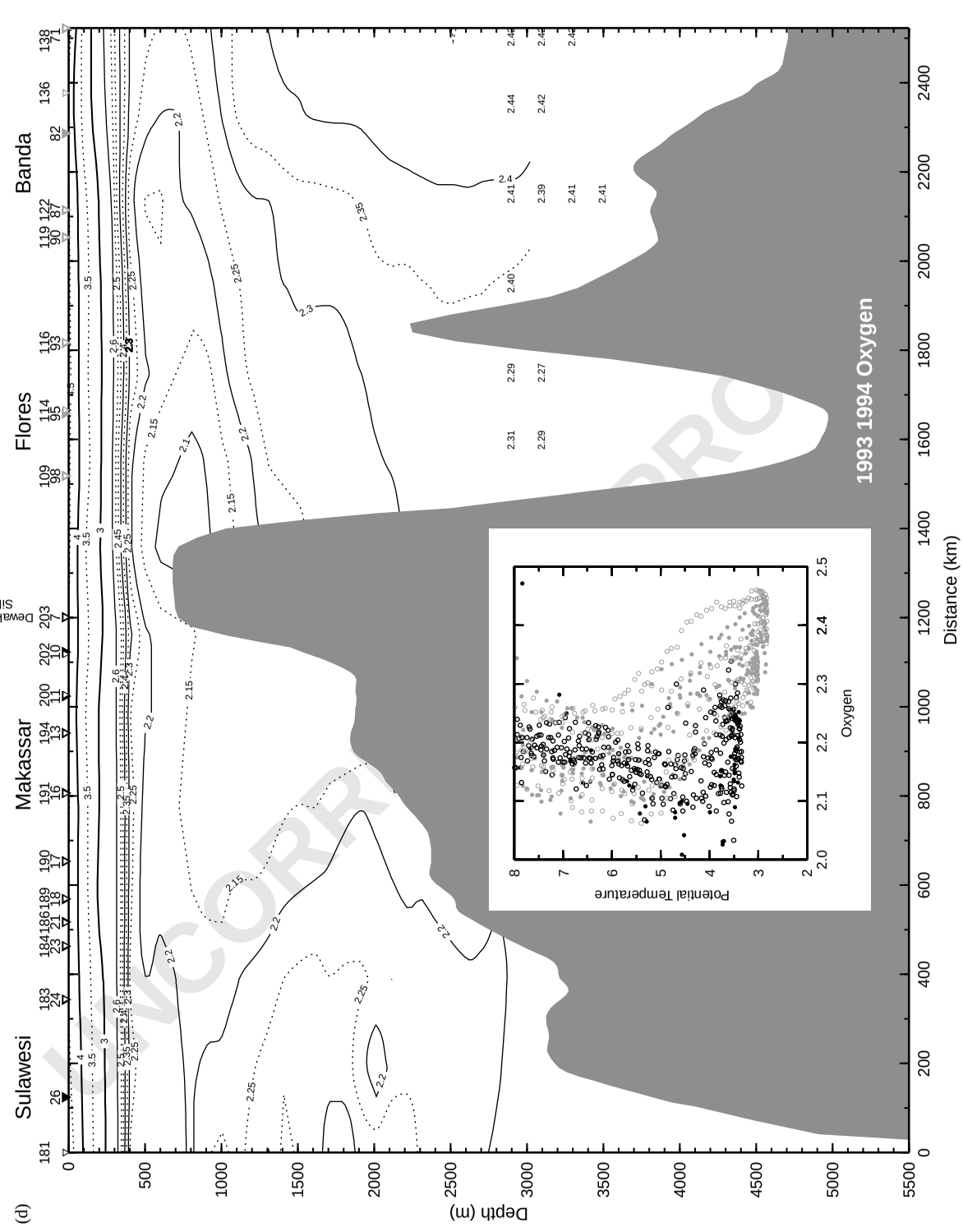

Fig. 5 (*continued*).

While the simple balance rigorously applies to the water column deeper than 1300 m, a reasonable exponential fit to the temperature profile occurs for the water column deeper than 300 m (Fig. 4). We fit an exponential to the interval 300–1500 m to determine the scale height for the depth range above the export of Lifamatola overflow (Table 3). The average scale height Z^* is 477 m. To convert Z^* to a mixing coefficient requires knowledge of the upwelling rate (or conversely knowledge of K_z is needed to calculate upwelling). Above the confines of the isolated Banda Basin the vertical velocity is not known. Therefore, a reasonable range of vertical velocities is offered. If the Lifamatola overflow upwelling value is applied across the full 300–1500 m interval, the resultant K_z is $11.4 \times 10^{-4}\,m^2/s$. If the Ekman-induced upwelling in the Banda Sea average of $1.39 \times 10^{-6}\,m/s$, upwelling value nominally at 100 m (Gordon and Susanto, 2001), is applied across the full 300–1500 m range, the K_z is $6.6 \times 10^{-4}\,m^2/s$.

The canonical K_z value of $1 \times 10^{-4}\,m^2/s$ implies an average upwelling of $0.21 \times 10^{-6}\,m/s$. While the thermocline is in the 100–200 m interval, shallower than the exponential profile, the use of a typical thermocline K_z value of $0.1 \times 10^{-4}\,m^2/s$ (Ledwell et al., 1993, 1998) results in an upwelling rate of $0.21 \times 10^{-7}\,m/s$. Alford et al. (1999) find $K_z = 0.92 \times 10^{-4}\,m^2/s$ in the Banda Sea near 100 m depth averaged over a 2 week cruise, but that period was one of minimal tidal activity, which may boost diapycnal mixing. (Ffield and Gordon, 1992, 1996).

4. Intra-basin exchange and subthermocline water masses

For completeness we offer sections of temperature, salinity and oxygen composed of August 1993 and February 1994 Arlindo data (Fig. 1) supplemented with data below 3000 m depth drawn from archived data (Conkright et al., 1998), for the western and eastern ITF paths. The western section (Fig. 5) stretches from the Sulawesi Sea, through the Makassar Strait and Flores Sea and into the southern Banda Sea. This is considered to be the main ITF path for thermocline water. The eastern section (Fig. 6) transverses the region from the Maluku Sea, the Seram Sea, into Banda Sea where it crosses the western pathway section, extending into the Timor Sea and Indian Ocean. The thermocline stratification based on the Arlindo data is described by Ilahude and Gordon (1996a, 1996b), Ffield and Gordon (1992) and archived data by Hautala et al. (1996), and will not be repeated here. The focus of this work is on the deeper, subthermocline stratification, supplementing the excellent series of papers derived from the Snellius II expedition of 1984–1985 (see Van Aken et al., 1988, 1991).

4.1. Western pathway

The controlling sill depth between Makassar Strait and the Flores Sea is the 680 m deep, rather broad, Dewakangs sill (Ilahude and Gordon, 1996a). As the deep water is ventilated by Pacific waters from both sides (from the Banda Sea fed by the Lifamatola Passage overflow and from the Sulawesi Sea fed by the Sangihe Ridge overflow), there is not a sharp discontinuity of stratification on either side of the Dewakang Sill. However, with increasing depth, differences in temperature and salinity as revealed in the θ/S scatter (Fig. 5b) begin to emerge near the 5.5°C (at 750 m), becoming more pronounced near 4.2°C (at 1200 m) with the Banda side being slightly saltier and cooler. During the southeast monsoon (August–September 1993; Fig. 5c) the deep water on the Makassar Strait side of Dewakang Sill is slightly (less than 0.01) fresher than that found during the northwest monsoon season of January–February 1994 (Fig. 5b).

The deep temperature and salinity indicate the presence of a deep topographic barrier of about 2300 m depth between the Banda Sea and Flores Sea. This sill blocks water colder than 3.0°C from flowing freely into the Flores Sea from the Banda Sea. Gordon et al. (1994; also see Top et al., 1997) describe a deep circulation pattern in the Flores Sea in which deep water from the Banda Sea, fed by Lifamatola overflow, spreads westward reaching the southern flank of Dewakang Sill, where it upwells and is returned to the east above 1200 m

UNCORRECTED PROOF

depth range, though some may occasionally overflow the Dewakang Sill into the southern Makassar Strait (an inference drawn from the Arlindo CFC, Waworuntu et al., 2000). The linear θ/S scatter between 4.2°C and 5.5°C represents a mixture of Banda deep and Makassar throughflow water. For water colder than the 4.2°C end-member the Flores Sea θ/S is identical to the Banda Sea deep water.

The oxygen distribution (Fig. 5d) shows that the deep water with the highest oxygen is found in the Banda Sea, roughly at 2000 m near the 3.1°C isotherm. This oxygen maximum slowly yields to lower values as the Banda Sea deep water spreads into the Flores Sea, though the Flores Sea deep water remains higher in oxygen than the deep water on the Makassar side of Dewakang Sill. The better-ventilated deep water is derived from the Lifamatola overflow. The lowest oxygen concentrations are found in Makassar Strait and between 500 and 2000 m in the Flores Sea. The oxygen distribution is consistent with the deep circulation scheme of the Flores Sea presented by Gordon et al. (1994) based on 1991 (pre-Arlindo) data.

4.2. Eastern pathway

The eastern path (Fig. 6) provides a deeper throughflow route than the western section. Below the thermocline South Pacific characteristics become more pervasive within the Indonesian seas as the main access path of North Pacific along the pathway is limited by the 680 m Dewakang Sill, and constituting the deep-water component of the throughflow (Wyrtki, 1961; Hautala et al., 1996).

Within the depth range from 200 to 600 m in the Maluku, Seram and to the northern boundary of the Banda Sea, a salinity maximum greater than 34.6 marks the signature of the South Pacific lower thermocline water (Gordon and Fine, 1996; Ilahude and Gordon, 1996a, b) into the Indonesian seas through the Halmahera Sea. It spreads both northward in the Maluku and southward into the Banda Sea, much more pervasion during the northwest monsoon phase (January/February 1994). In the central and southern Banda Sea the South Pacific lower thermocline water is replaced by the lower salinity North Pacific thermocline water drawn through the Makassar Strait.

Antarctic Intermediate Water is observed within the Maluku and Seram Seas as a salinity-minimum and oxygen-minimum between 600 and 1000 m. This core layer attenuates in the Seram Sea and disappears within the northern Banda Sea. Wyrtki (1961, Plates 28–30) does not show an Antarctic Intermediate Water spreading path from the Maluku Sea into the Banda Sea. The August/September 1993 low salinity (Fig. 6b) core layer near 700 m in the central and southern Banda Sea (stations 62–71) may also be a remnant of Antarctic Intermediate Water but it is not contiguous with the Maluku Sea Antarctic Intermediate Water salinity minimum. In February 1994 (Fig. 6c) the salinity pattern displays weakening of the vertical gradient in the 500–700 m interval. It is suggested that "trace" presence of Antarctic Intermediate Water in the central and southern Banda Sea is derived from the Makassar Strait, which is consistent with the thermocline flow lines presented by Gordon and Fine (1996).

The Lifamatola Passage surveyed sill depth is 1940 m (Van Aken et al., 1988), but the water spilling into the Seram and Banda Seas represents a mixture of the lower 500 m of the Lifamatola water column (Van Aken et al., 1988; Ffield and Gordon, 1996). This is due to mixing at the sill, as

Fig. 6. Eastern throughflow pathway. Vertical sections: (a) contours of potential temperature combining 1993 and 1994 Arlindo data, on the upper right, map showing the location of the section based on the Arlindo data and in small solid circles the location of the archived data, middle right potential temperature versus salinity for both 1993 and 1994 Arlindo data and on the lower right potential temperature versus oxygen for both 1993 and 1994 Arlindo data (b) contours of salinity only for 1993 Arlindo data; (c) contours of salinity for the upper 2500 m 1994 Arlindo data; (d) contours of oxygen (ml/l) combining 1993 and 1994 Arlindo data. The bottom topography along the section is generalized to show only the major basins and topographic barriers. The values shown in most of deep basins represent a spatial/temporal average of archived data (Conkright et al., 1998) found within 50 km from the cruise track. For all sections solid symbols represent Arlindo 1993 data and open symbols, Arlindo 1994 data.

UNCORRECTED PROOF

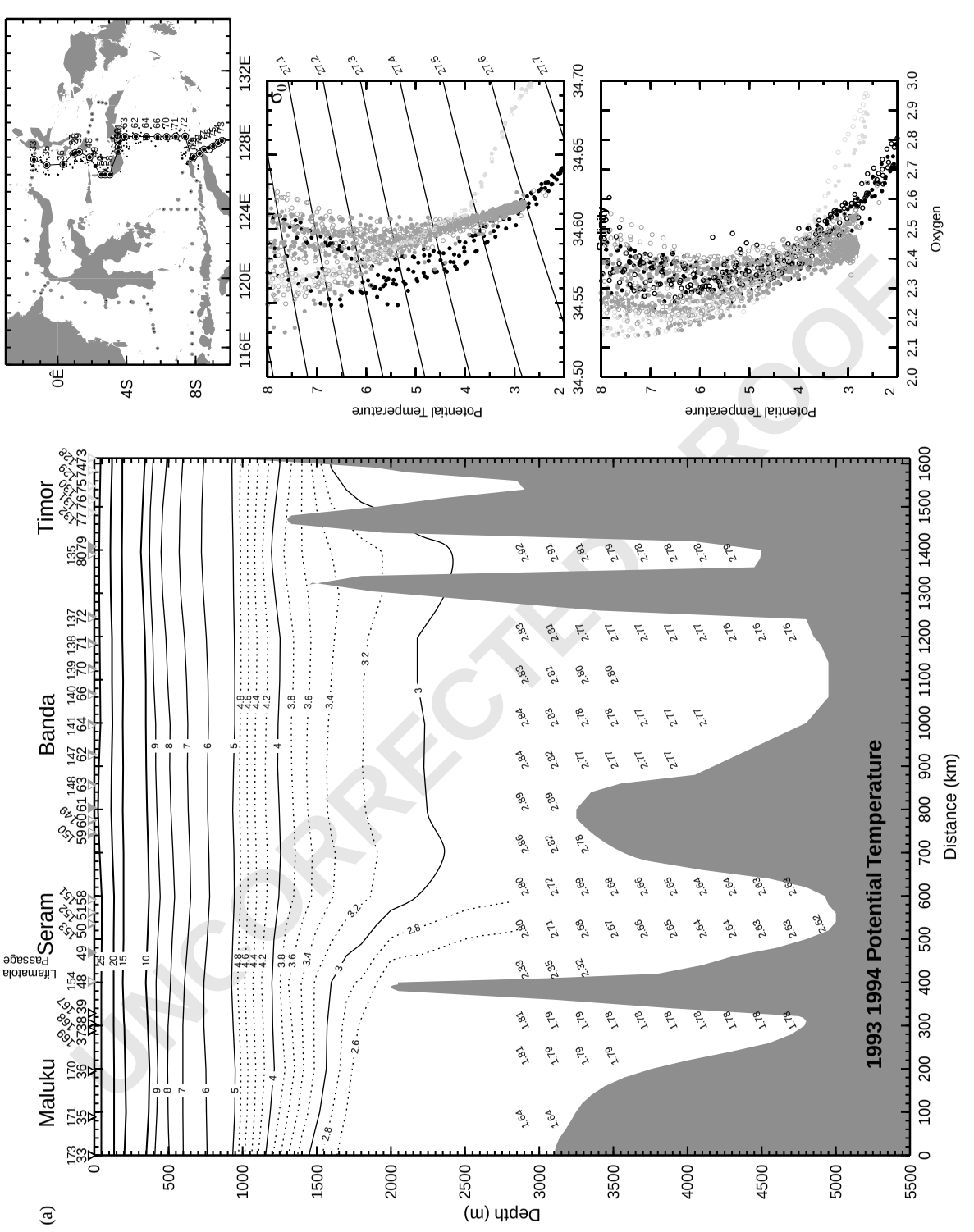

UNCORRECTED PROOF

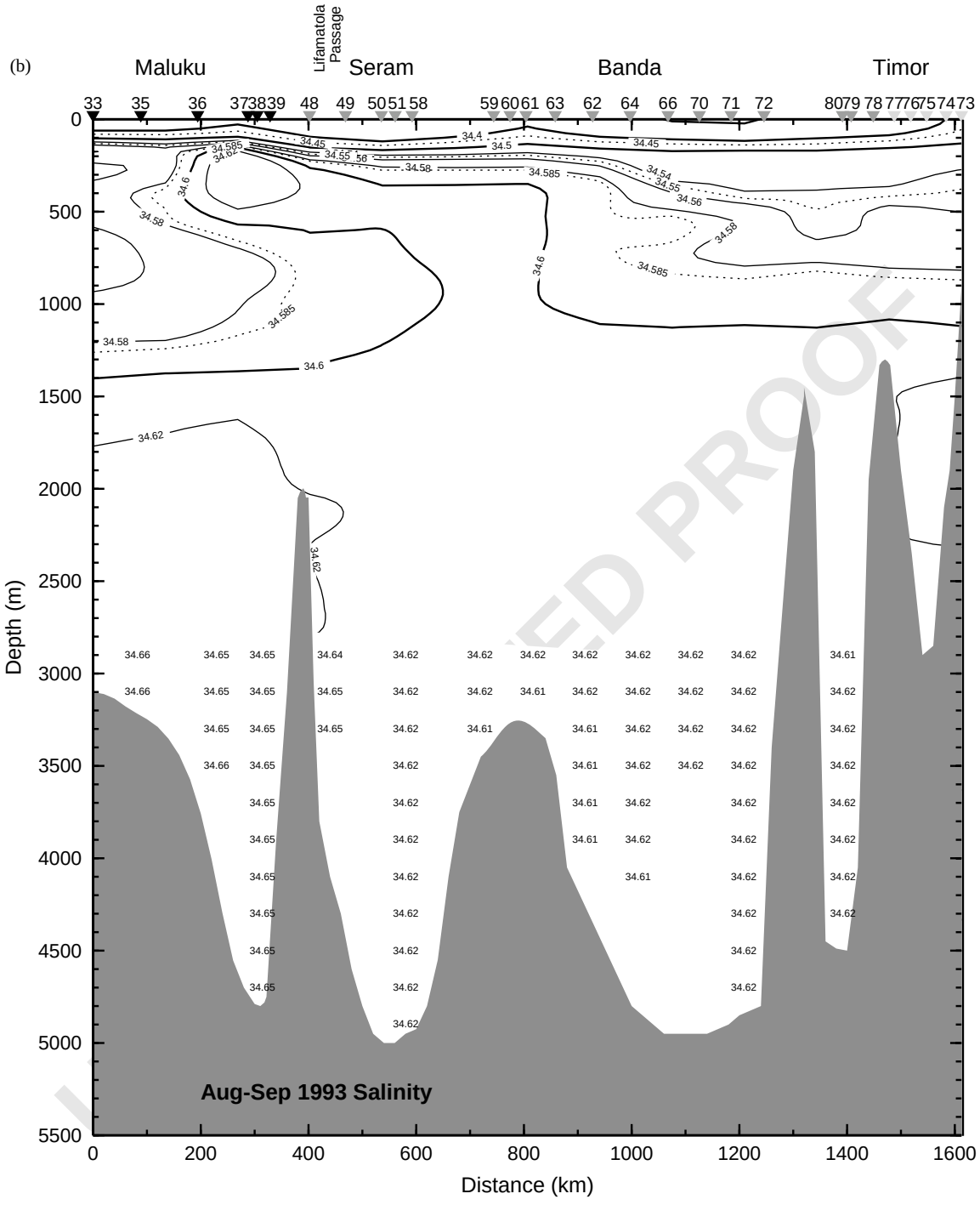

Fig. 6 (*continued*).

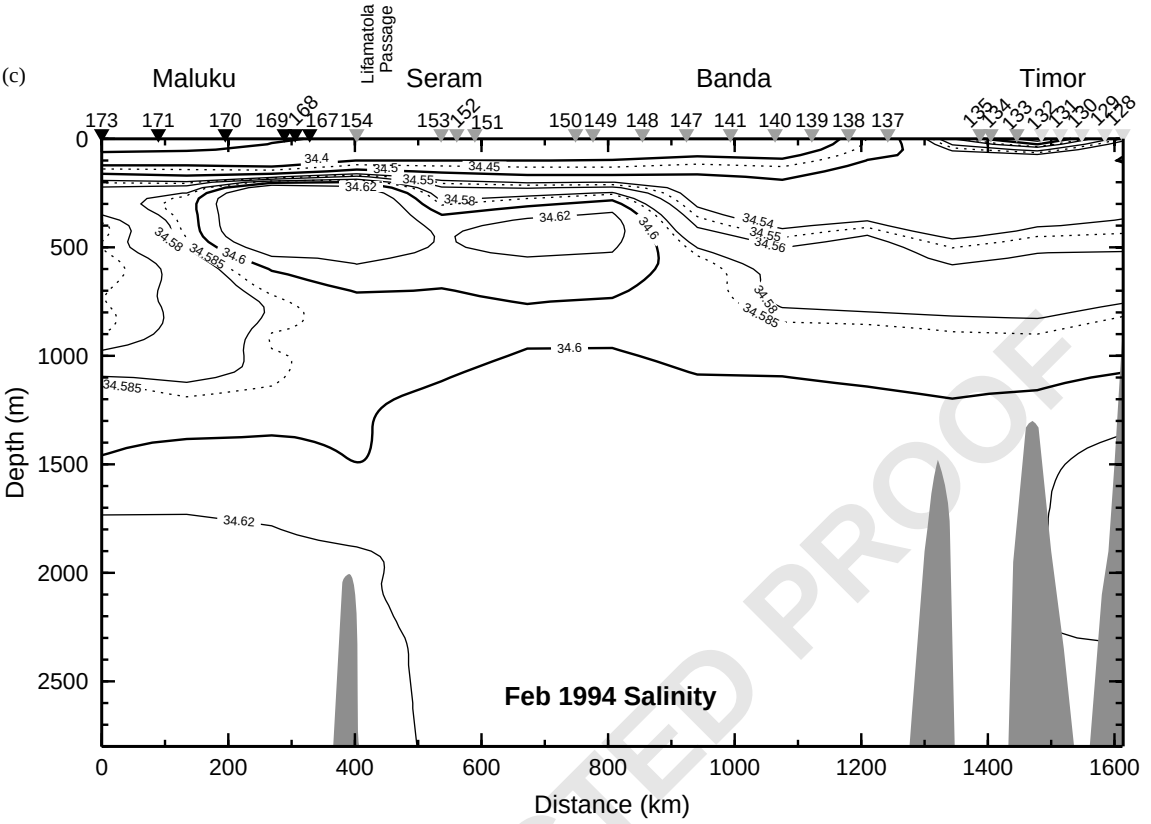

Fig. 6 (*continued*).

mentioned above. The Arlindo data suggest that this is a variable process. Stations 48 (August 1993, Fig. 6a; latitude: 1.846°S, longitude: 126.994°E, close to the Lifamatola sill; station 48 deepest measurement is at 1990 m with a water depth of 2122 m) and 154 (February 1994, Fig. 6a; latitude: 1.848°S; longitude: 126.993°E; station 154 deepest measurement is at 2029 m with a water depth of 2045 m) are in the Lifamatola Passage, slightly on the Seram Sea "spill-over" side of the passage. They show significantly different bottom temperature. The bottom potential temperature at station 48 is 2.714°C, but at station 154 it is 2.460°C, a difference of 0.25°C. The bottom temperature of the Banda Sea from the archived data is 2.78°C, close to the bottom temperature at station 48. Fluctuating in overflow temperature may be a product of internal waves and tides, which produce heave of the isopycnals at the sill depth. The average overflow, over the 40-year residence time of the Banda Sea, is responsible for the mean overflow temperature of 2.78°C.

The Seram and Banda seas display an oxygen maximum from 2000 to 2600 m. A possible explanation is as follows. Relatively high-oxygen water at the Lifamatola sill overflows into the deep Banda Sea and then upwells slowly within the confines of the deep basin as required to balance downward eddy diffusion of buoyancy and "make room" for continued overflow from Lifamatola. At the shallower level of the confined basin the lowest oxygen is expected, as this water has been in resident for the longest time. However, in the Banda Sea, above the Lifamatola sill depth, relatively oxygenated water spreads southward from the Maluku Sea on a more horizontal plane

UNCORRECTED PROOF

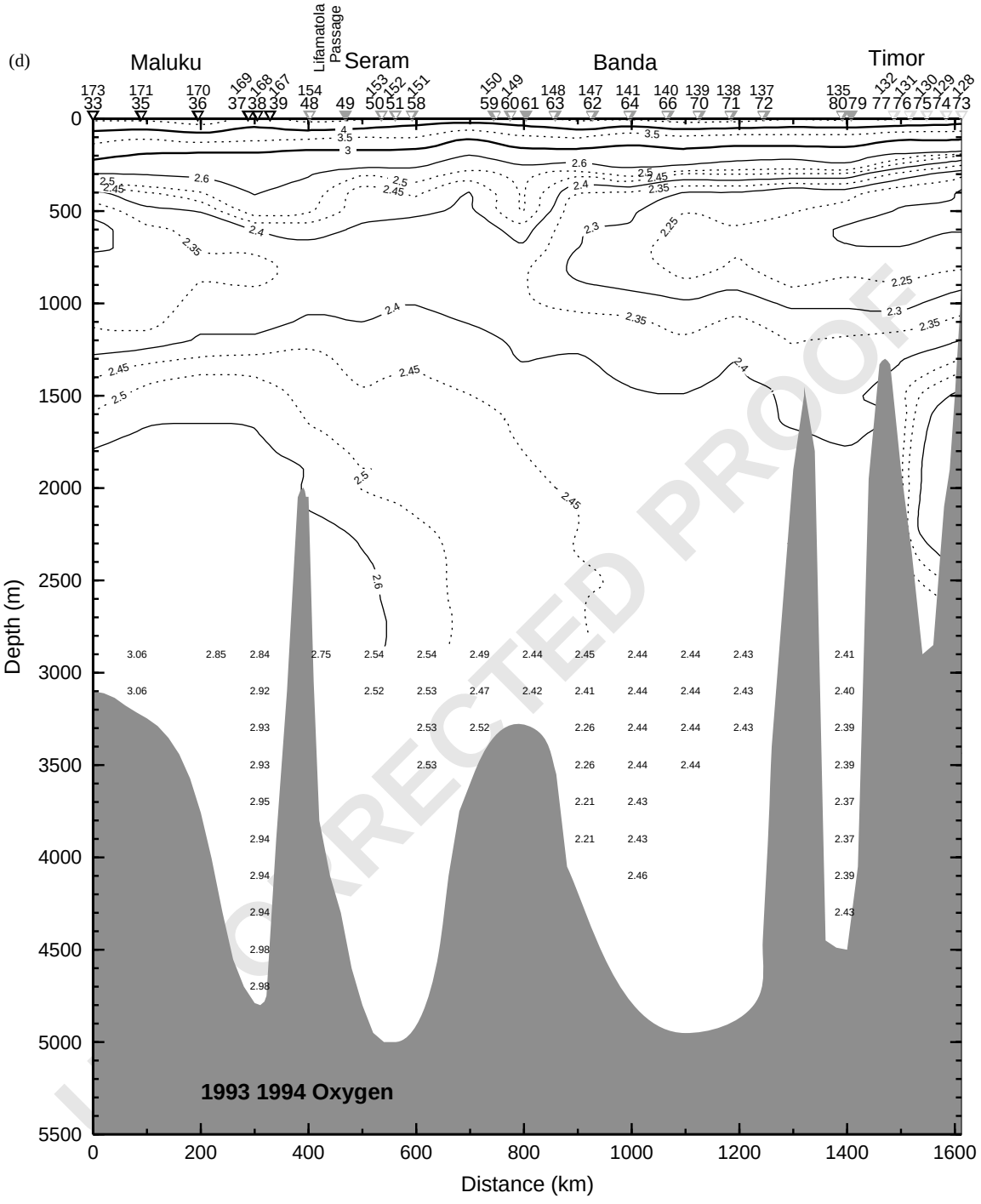

Fig. 6 (*continued*).

UNCORRECTED PROOF

into the Banda Sea, producing a slight oxygen maximum near and slightly shallower than the controlling sill depth.

5. Summary

Transfer of water from the Pacific Ocean to the Indian Ocean through the Indonesian seas is accomplished mainly in the thermocline layer (Gordon et al., 1999). However, water properties reveal significant contribution to the interocean throughflow may be derived from the deeper layer. Below the thermocline numerous topographic barriers or sills separating the basins of the Indonesian seas impede throughflow. This results in a deep circulation pattern governed by density-driven overflow processes. While a few sills have been surveyed by sonic means, most have not. For these comparison of temperature and salinity of the water column on either side of a sill allow estimation of the effective depth of the sill.

Pacific water may follow three possible paths into the northern Indonesian seas. A 1350 m deep sill in the Sangihe Ridge blocks flow into the Sulawesi Sea. The shallowest barrier is found between the Halmahera Sea and Seram Sea, with a sill depth of 580 m. The deepest is occurs between the Maluku Sea and the Seram Sea, within the Lifamatola Passage, with a depth of 1940 m. Escape to the Indian Ocean occurs over the Sunda Arc. The deepest sill is near Timor and is estimated to be from 1300 to 1450 m deep, possibly as deep as 1500 m. However, the bulk of the throughflow does not necessarily follow the deepest route. The main throughflow path is accomplished within the thermocline layer passing through the Makassar Strait. The southern end of the Makassar Strait is marked by a relatively shallow sill, the 680-m-deep Dewakang Sill, which limits the continuation of throughflow into the Flores Sea. Some throughflow water escapes to the Indian Ocean through the 300 m deep Lombok Strait, but most passes to the Banda Sea to cross into the Indian Ocean over the deeper gaps of the Lesser Sunda Arc near Timor. Throughflow water found deeper than roughly 680 m must enter the Banda Sea from the eastern channels, including overflow within the Lifamatola Passage.

Using transport values obtained at various sites, at different times, an approximate balance of the inflow and outflow of Indonesian waters is found. Export to the Indian Ocean of 7.3–10.7 Sv is suggested for the water column shallower than 680 m (Dewakang Sill). Below 680 m the export in the passage on either side of Timor is estimated as 1.8–2.3 Sv, which matches the estimated flow though Lifamatola Passage.

Water overflowing into the depths of an isolated basin displaces the residence water made less dense by vertical mixing processes (and perhaps geothermal heat flux). In this way the density-driven overflow is balanced by compensated upwelling within the confines of the basins. The profiles of temperature within the deep Banda and Seram Seas conform very closely to an exponential form, which is expected from a simple vertical balance of upwelling with vertical mixing. A scale depth (Z^*) of 477 m is characteristic of the 300–1500 m depth range, with a value of 565 m for the water column deeper than 1300 m. Deep vertical mixing coefficients as high as $10–15 \times 10^{-4}$ m^2/s are implied.

6. Uncited reference

Fieux et al., 1994.

Acknowledgements

Analysis of the Arlindo data set is derived from NSF Grant OCE00-99152. We are greatly appreciative of the comments of the anonymous reviewers whose careful reading and insightful comments improved the manuscript.

References

Alford, M., Gregg, M., Ilyas, M., 1999. Diapycnal mixing in the Banda Sea: results of the first microstructure measurements in the Indonesian throughflow. Geophysical Research Letters 26, 2741–2744.

UNCORRECTED PROOF

Berger, G.W., Van Bennekom, A.J., Kloosterhuis, H.J., 1988. Radon profiles in the Indonesian archipelago. Netherlands Journal of Sea Research 22, 395–402.

Broecker, W.S., Patzert, W.C., Toggweiler, R., Stuiver, M., 1986. Hydrography, chemistry and radioisotopes in the southeast Asian basins. Journal of Geophysical Research 91 (C12), 14345–14354.

Conkright, M.E., Levitus, S., O'Brien, T., Boyer, T.P., Antonov, J.I., Stephens, C., 1998. World ocean atlas CD-ROM data set documentation. NODC Internal Report 15, Silver Spring, MD, 16pp.

Ffield, A., Gordon, A.L., 1992. Vertical mixing in the Indonesian thermocline. Journal of Physical Oceanography 22 (2), 184–195.

Ffield, A., Gordon, A., 1996. Tidal mixing signatures in the Indonesian seas. Journal of Physical Oceanography 26, 1924–1937.

Fieux, M., Andrie, C., Charriaud, E., Ilahude, A.G., Metzl, N., Molcard, R., Swallow, J., 1996. Hydrological and chloroflоromethane measurements of the Indonesian throughflow entering the Indian Ocean. Journal of Geophysical Research 101 (C5), 12433–12454.

Fieux, M., Andrié, C., Delecluse, P., Ilahude, A.G., Kartavtseff, A., Mantisi, F., Molcard, R., Swallow, J.C., 1994. Measurements within the Pacific–Indian Ocean throughflow region. Deep-Sea Research 41 (7), 1091–1130.

Gordon, A.L., 1995. When is "appearance" reality? Indonesian throughflow is primarily derived from north Pacific water masses. Journal of Physical Oceanography 25 (6), 1560–1567.

Gordon, A.L., Fine, R.A., 1996. Pathways of water between the Pacific and Indian oceans in the Indonesian seas. Nature 379, 146–149.

Gordon, A.L., McClean, J., 1999. Thermohaline stratification of the Indonesian seas, model and observations. Journal of Physical Oceanography 29, 198–216.

Gordon, A.L., Susanto, R.D., 2001. Banda Sea surface layer divergence. Ocean Dynamics 52, 2–10.

Gordon, A., Ffield, A., Ilahude, A.G., 1994. Thermocline of the Flores and Banda seas. Journal of Geophysical Research 99 (C9), 18235–18242.

Gordon, A.L., Susanto, R.D., Ffield, A.L., 1999. Throughflow within Makassar Strait. Geophysical Research Letters 26, 3325–3328.

Hautala, S., Reid, J., Bray, N., 1996. The distribution and mixing of Pacific water masses in the Indonesian seas. Journal of Geophysical Research 101 (C5), 12375–12389.

Ilahude, A.G., Gordon, A.L., 1996a. Water masses of the Indonesian seas throughflow. Proceedings IOC-WESTPAC Third International Scientific Symposium, Bali, Indonesia, 22–26 November 1994, pp. 572–587.

Ilahude, A.G., Gordon, A.L., 1996b. Thermocline stratification within the Indonesian seas. Journal of Geophysical Research 101 (C5), 12401–12409.

Ledwell, J., Watson, A., Law, C., 1993. Evidence for slow mixing across the pycnocline from an open-ocean tracer-release experiment. Nature 364, 701–703.

Ledwell, J.R., Watson, A.J., Law, C., 1998. Mixing of a tracer in the pycnocline. Journal of Geophysical Research 103 (C10), 21499–21530.

Mammericks, J., Fisher, R., Emmel F., Smith, S., 1976. Bathymetry of the east and southeast Asian Sea. Scripps Institution of Oceanography.

Molcard, R., Fieux, M., Ilahude, A.G., 1996. The Indo-Pacific throughflow in the Timor passage. Journal of Geophysical Research 101 (C5), 12411–12420.

Molcard, R.M., Fieux, M., Syamsudin, F., 2001. The throughflow within Ombai Strait. Deep-Sea Research 48, 1237–1253.

Munk, W.H., 1966. Abyssal recipes. Deep-Sea Research 13, 707–730.

Murray, S.P., Arief, D., 1988. Throughflow into the Indian Ocean through the Lombok Strait, January 1985–January 1986. Nature 333, 444–447.

Murray, S.P., Arief, D., Kindle, J.C., 1990. Characteristics of circulation in an Indonesian archipelago strait from hydrography, current measurements and modeling results. In: Pratt, L. (Ed.), The Physical Oceanography of Sea Straits. Kluwer Academic Publishers, Norwell, MA, pp. 3–23.

Postma, H., Mook, W.G., 1988. The transport of water through the east Indonesian deep sea water. Netherlands Journal of Sea Research 22, 373–381.

Smith, W., Sandwell, D., 1997. Global sea floor topography from satellite altimetry and ship depth soundings. Science 277 (5334), 1956–1962.

Top, Z., Gordon, A., Jean-Baptiste, P., Fieux, M., Ilahude A, .G., Muchtar, M., 1997. ^{3}He in Indonesian seas: inferences on deep pathways. Geophysical Research Letters 24 (5), 547–550.

Van Aken, H.M., Punjanan, J., Saimima, S., 1988. Physical aspects of the flushing of the East Indonesian basins. Netherlands Journal of Sea Research 22, 315–339.

Van Aken, H.M., Van Bennekom, A.J., Mook, W.G., Postma, H., 1991. Application of Munk's abyssal recipes to tracer distributions in the deep waters of the southern Banda basin. Oceanologica Acta 14 (2), 151–162.

Van Bennekom, A., 1988. Deep-water transit times in the eastern Indonesian basins, calculated from dissolved silica in deep and interstitial waters. Netherlands Journal of Sea Research 22 (4), 341–354.

Waworuntu, J., Fine, R., Olson, D., Gordon, A., 2000. Recipe for Banda Sea water. Journal of Marine Research 58, 547–569.

Wolanski, E., Ridd, P., Inoue, M., 1988. Currents through Torres Strait. Journal of Physical Oceanography 18 (11), 1535–1545.

Wyrtki, K., 1961. Physical oceanography of the southeast Asian Waters, NAGA Rep. 2, Scripps Institution of Oceanography.

UNCORRECTED PROOF